

ELECTRON AND HOLE MOBILITY REDUCTION AND HALL FACTOR IN PHOSPHORUS-COMPENSATED P-TYPE SILICON

F. E. Rougieux¹, D. Macdonald¹, A. Cuevas¹, S. Ruffell², J. Schmidt³, B. Lim³ and A. P. Knights⁴

¹School of Engineering, The Australian National University, Canberra, ACT 0200, Australia

²Department of Electronic Materials Engineering, The Australian National University, Canberra ACT 0200, Australia

³Institut für Solarenergieforschung Hameln (ISFH), Am Ohrberg 1, D-31860 Emmerthal, Germany

⁴McMaster University, 1280 Main Street West, Hamilton, Ontario, Canada L8S 4L7

ABSTRACT: The conductivity mobility for majority carrier holes in compensated p-type silicon is determined by combined measurement of the resistivity and the net doping, the latter via electrochemical capacitance-voltage measurements. The minority electron mobility was also measured with a technique based on measurements of surface-limited effective carrier lifetimes. While both minority and majority carrier mobilities are found to be reduced by compensation, the impact is greater on the minority electron mobility. The Hall factor, which relates the Hall mobility to the conductivity mobility, has also been determined using the Hall method combined with the capacitance-voltage measurements. Our results indicate a similar Hall factor in both compensated and non-compensated samples.

1. INTRODUCTION

A large amount of experimental data and numerous models concerning mobilities in non-compensated silicon exist in the literature.[1-9] This allows one to easily deduce the bulk dopant density from resistivity data, for example. Knowing the dopant density one can also predict the minority and majority carrier mobility for a wide range of temperatures and injection levels, and thus characterize and simulate the behaviour of solar cells or other devices under various conditions.

Solar-grade silicon often contains high concentrations of both acceptors and donors. Such dopant compensation reduces the net doping ($p_0 = N_A - N_D$ for p-type silicon) and thus increases the resistivity ($\rho = 1/qp_0\mu_p$). For the same resistivity, a compensated sample will therefore have more ionised impurities than a non-compensated sample. The resulting greater ionised impurity scattering can be expected to reduce the mobility in the compensated sample.[10] Previous measurements using Free Carrier Absorption,[11] Capacitance Voltage[12-14], Glow Discharge Mass Spectroscopy,[15] or the Hall method[12, 16, 17] have shown that the majority carrier mobility in silicon is affected by compensation. Other measurements in compensated germanium have shown a similar trend for majority carriers[18, 19] and minority carriers[20].

The increased impurity concentration and the different scattering properties of ionised acceptors and donors are only two of the peculiarities that make carrier mobilities in compensated silicon intriguing. Another interesting aspect is that the effect of compensation is not the same for electron and holes. In p-type compensated silicon, even though both electrons and holes will be scattered by more impurities (N_A and N_D), they will also see *fewer* free holes. The lower hole concentration will result in lower hole-hole screening and lower electron-hole scattering. This means that while the higher impurity concentration reduces the electron mobility, the lower free hole concentration will tend to increase the electron mobility. The problem of mobility in compensated silicon is thus not straightforward, and experimental data for both majority and minority carrier mobility are needed to ascertain the degree of impact of the various scattering mechanisms.

In this paper, the majority hole conductivity mobility, which is essential to deduce the bulk net doping p_0 from resistivity ρ measurements, is measured for different acceptor and donor concentrations.

As solar cells are minority carrier devices, it is also of fundamental importance to assess the minority carrier mobility in compensated silicon. Diffusion lengths have been measured in compensated silicon before [15, 17, 21, 22] but until now, no direct experimental data concerning minority electron mobility in compensated p-type silicon has been measured.

A common method for measuring the majority carrier mobility is the Hall method. Unfortunately, the Hall method requires knowledge of the Hall factor in order to convert the Hall mobility into the conductivity mobility, which is the parameter of interest for solar cell operation. The Hall Factor has been measured before in low purity compensated silicon [23] and in lightly doped silicon highly compensated with thermal donors.[12] In our study, the Hall factor is determined by a direct comparison between independent measurements of the Hall mobility and conductivity mobility on the same samples (boron and phosphorus doped).

Finally, it is also of interest for further simulation and characterization to know if conventional mobility models such as Klaassen's[2, 3] model can be used safely for compensated silicon. We therefore compare Klaassen's model with our experimental results to assess its accuracy.

2. SCATTERING MECHANISMS

Solar cells are low electric field devices, and the carrier mobility of interest in solar cells is the bulk mobility. Various scattering mechanisms contribute to limit the bulk carrier mobility in silicon. These include defect scattering (crystal defects, dopants, impurities), carrier-carrier scattering and lattice scattering (intra and intervalley[24]). Hole-hole ($\mu_{h,h}$) and electron-electron ($\mu_{e,e}$) scattering can not alter the total momentum but can increase the momentum transfer rate,[25] as such they only represent a second order effect on the mobility.[2, 3]

In single crystal silicon at room temperature, crystal defects are insignificant in terms of carrier scattering, and

the bulk mobility of electrons and holes has previously been shown to be mainly affected by ionized donor and acceptor impurity scattering ($\mu_{e,D}$, $\mu_{e,A}$, $\mu_{h,D}$, $\mu_{h,A}$), electron-hole scattering ($\mu_{e,h}$, $\mu_{h,e}$) and lattice scattering ($\mu_{e,L}$, $\mu_{h,L}$). [3] Using Matthiesen's rule, the total mobility is given by the sum of these terms: [2, 3]

$$\frac{1}{\mu_h} = \frac{1}{\mu_{h,L}} + \frac{1}{\mu_{h,D}} + \frac{1}{\mu_{h,A}} + \frac{1}{\mu_{h,e}} \quad (1)$$

$$\frac{1}{\mu_e} = \frac{1}{\mu_{e,L}} + \frac{1}{\mu_{e,D}} + \frac{1}{\mu_{e,A}} + \frac{1}{\mu_{e,h}} \quad (2)$$

How will compensation affect these various scattering mechanisms? Figures 1 and 2 show the contribution of all these mechanisms in compensated p-type silicon for various compensation ratios ($R_C = (N_A + N_D)/(N_A - N_D)$). From $R_C=1$ (non-compensated, $N_D=0$ cm⁻³) to $R_C=100$ (nearly fully-compensated, $N_D=0.98 \times N_A$) the graphs show the effect of introducing donors at a fixed acceptor concentration ($N_A=1 \times 10^{17}$ cm⁻³). The mobilities are simulated with Klaassen's mobility model. [2, 3] Figure 1 shows the majority hole mobility. The compensated donors are ionised at room temperature and thus act as additional ionised scattering centres, reducing the mobility. For increasing donor concentration (increasing compensation), the acceptor scattering mechanism becomes slightly less effective. This is due to screening of acceptors by donors. This means that acceptors are more effective scattering centres for very low compensation ratio. Near full compensation ($R_C=100$), the effect of the acceptor and donor becomes similar. The global result of the three scattering mechanisms shown in Fig. 1 is that the majority carrier (hole) mobility is only very slightly reduced by compensation. This is due to the fact that in this example the dominant mechanism is lattice scattering.

Figure 2 corresponds to the minority electron mobility. Because electrons are minority carriers they see many

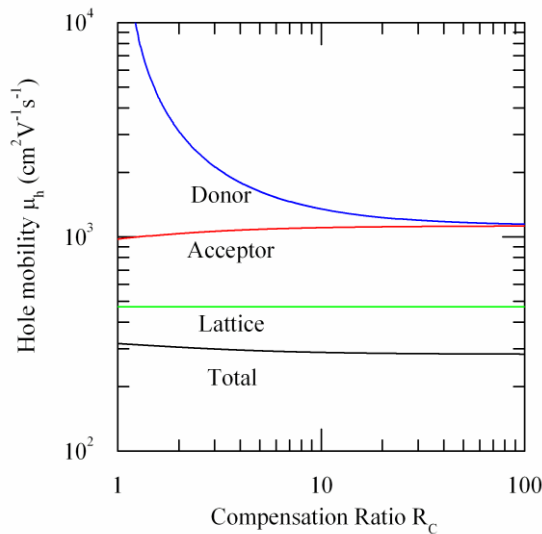


Figure 1: Majority hole mobility as a function of compensation ratio for silicon with $N_A=1 \times 10^{17}$ cm⁻³, the contributions of the various scattering mechanisms are shown.

holes, whereas holes virtually see no electrons ($p \times n = n_i^2$). This means that electron-hole scattering is a significant scattering mechanism reducing minority electron mobility in lowly-compensated materials ($R_C < 3$ in Fig.2). In compensated silicon the hole concentration is reduced, leading to a strong reduction of the electron-hole scattering. The contribution of the electron-hole scattering on the total minority carrier mobility becomes negligible. Nevertheless, this effect is not sufficient to counteract the additional donor scattering, and so the minority electron mobility still decreases slightly with compensation. The total carrier mobility in Figs 1 and 2, showing only a small dependence on R_C , may lead one to believe that compensation does not have a significant impact on mobility. This is true in the sense of the addition of donors to a given acceptor concentration not altering the mobility much. However, the addition of donors produces a tremendous change on the free carrier density and hence on the resistivity. If a comparison was made between silicon of the same resistivity, one compensated and the other not, then the impact of compensation on carrier mobility would be larger. This is the type of comparison most commonly done in practice.

3. EXPERIMENTAL METHODS

The samples used in these studies were 155×155 mm pseudo-square, p-type, <100>-oriented Czochralski-grown silicon wafers with random pyramid texture. The samples came from three control ingots (non-compensated), which were boron-doped, with sample resistivities of 4.78 Ωcm, 1.28 Ωcm and 0.48 Ωcm, and from two compensated ingots, doped with both boron and phosphorus, with sample resistivities of 1.14 Ωcm and 0.43 Ωcm. For more details regarding these samples see Ref. 23. The acceptor concentrations N_A were previously determined using a method based on the association time constant of iron-boron pairs. [26] The donor concentrations N_D were determined using net dopant densities measured by

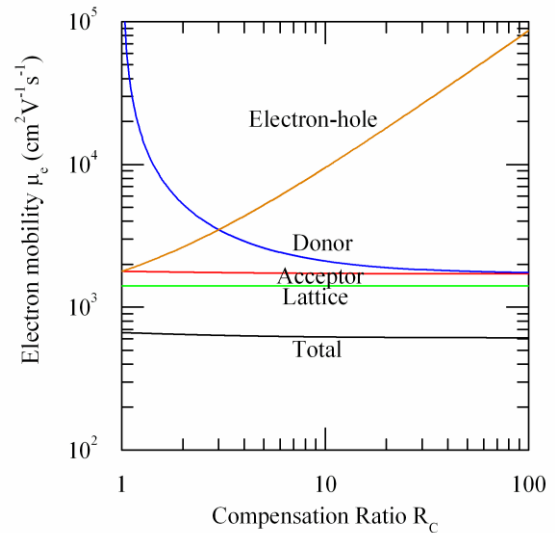


Figure 2: Minority electron mobility as a function of compensation ratio for silicon with $N_A=1 \times 10^{17}$ cm⁻³, the contributions of the various scattering mechanisms are shown

Table I. Measured and modelled (Klaassen) minority and majority carrier mobility in compensated and non-compensated silicon

ρ (Ωcm)	Concentration (cm^{-3})			Measured mobility ($\text{cm}^2\text{V}^{-1}\text{s}^{-1}$)			Klaassen mobility ($\text{cm}^2\text{V}^{-1}\text{s}^{-1}$)	
				Majority		Minority	Majority	Minority
	N_A	N_D	p_0	Hall	Conductivity			
				p-type control				
4.70	2.10×10^{15}	-	2.10×10^{15}	316	-	-	456	1283
1.28	1.15×10^{16}	-	1.15×10^{16}	281	435 ± 13	1120 ± 100	425	1082
0.48	3.50×10^{16}	-	3.50×10^{16}	246	372 ± 11	765 ± 80	382	878
				p-type compensated				
1.14	4.00×10^{16}	2.5×10^{16}	1.50×10^{16}	244	365 ± 11	660 ± 57	358	838
0.53	8.10×10^{16}	4.05×10^{16}	4.05×10^{16}	218	291 ± 9	476 ± 87	315	684

Electrochemical Capacitance Voltage (ECV) combined with acceptor density values, via $N_D = N_A - p_0$, and as listed in Table I.

All the samples were surface etched to remove the pre-existing random pyramid texture. The samples were cut in $1 \times 1 \text{ cm}^2$ pieces using a dicing saw. Aluminium contacts were then evaporated at each corner of the samples according to the Van der Pauw structure.[27] The resistivity (ρ) was measured using a four point probe setup on the four aluminium contacts.

The conductivity carrier concentration ($p_{0,C}$) was then measured on the same samples using a CPV21 ECV profiler with contact on the Al pads. The area of the ECV crater was measured externally by a pin profiler (Dektak). This allowed for the correction of the calculated dopant density as explained by *Bock et al.*[28] The profile was found to stabilize after $0.1 \mu\text{m}$. To minimize the uncertainty, more than 30 net dopant measurements were made until a depth of $0.4\text{-}0.5 \mu\text{m}$ was reached. The dopant density value was determined as the mode of the net dopant values. By avoiding the use of the average value, the initial measurements and the local false measurements (mainly due to bubbles in the electrolyte) were excluded. The conductivity mobility was then calculated ($\mu_C = 1/q p_{0,C} \rho$).

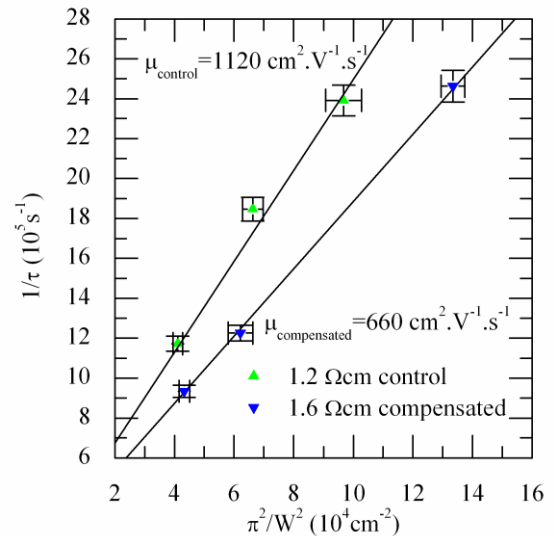
In order to perform minority carrier mobility measurements with the technique developed by Sproul *et al.*[29] further $155 \times 155 \text{ mm}$ square wafers were cut into $4 \times 4 \text{ cm}^2$ pieces. The wafers were then etched to different thicknesses ranging from $90 \mu\text{m}$ to $170 \mu\text{m}$ using a standard $\text{HNO}_3\text{:HF}$ etch. This tends to yield non uniform surface thickness near the edges. Nevertheless the $2 \times 2 \text{ cm}^2$ central part was found to be uniform in thickness. The surfaces were next abraded to yield infinite surface recombination velocities. The effective lifetimes were then dominated by surface recombination, and their magnitudes determined by the diffusivity (or mobility) of minority carriers, as described below.

These lifetimes were measured using the microwave photoconductance decay (MW-PCD) technique with an excitation wavelength of 904 nm . This is the same wavelength used by *Sproul et al.*[29] The lifetime variation due to increasing laser power was monitored in order to achieve a high signal/noise ratio without reaching high-injection conditions, which would affect the mobility.

The lifetime was measured more than 25 times with averaging over 1024 pulses to get a low standard deviation.

Figure 3 shows the reduction of the measured effective lifetime with thickness, plotted in the manner used by Sproul, allowing the minority carrier electron mobility to be determined on each of the samples. The uncertainty in the mobilities was estimated using a best fit within the error bars of the $1/\tau$ vs $(\pi/W)^2$ data (with W the sample thickness).

The Hall carrier concentration ($p_{0,H}$) was then measured on the Van der Pauw structure using an Accent HL5500PC Hall Effect measurement system with a magnetic field strength of 0.32T (low magnetic field). This allowed for the determination of the Hall mobility ($\mu_H = 1/q p_{0,H} \rho$). Using both Hall and conductivity measurements allows us to determine the Hall mobility and the conductivity mobility, and therefore the Hall factor. By making both carrier concentration measurements at the same place on the same sample, we avoid any uncertainty due to dopant differences between samples.


Figure 3: Plot of $1/\tau$ vs $(\pi/W)^2$ to determine the minority carrier mobility. The error in the mobility is determined using the best fit within the error bars

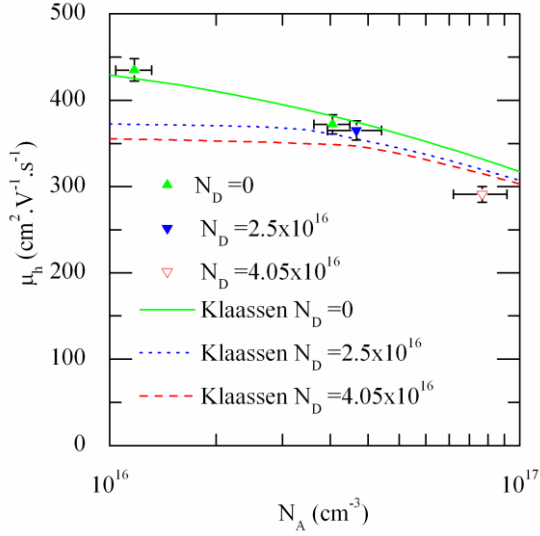


Figure 4: Majority conductivity hole mobility in compensated and non-compensated p-type silicon versus acceptor concentration for different donor concentrations

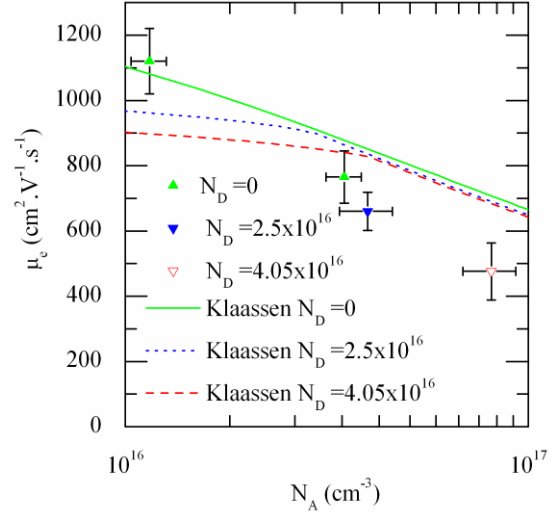


Figure 5: Minority electron mobility in compensated and non-compensated p-type silicon versus acceptor concentration for different donor concentrations

4. RESULTS AND DISCUSSION

4.1. Majority carrier conductivity mobility

The majority hole conductivity mobilities determined by ECV and resistivity measurements are listed in Table I for two control samples and the two compensated samples. Note that these four samples occur in two pairs with similar values of p_0 , which provides a useful basis for comparison. The results reveal a 15-20% reduction of the hole mobility in the compensated silicon wafers compared to non-compensated silicon samples with similar net doping. For both the controls and the compensated samples the measured values are in very good agreement with those predicted by *Klaassen's* model.

The results are also plotted in Figure 4, as a function of the acceptor concentration N_A . *Klaassen's* model is shown for three cases, with $N_D=0$ cm⁻³, $N_D=2.5 \times 10^{16}$ cm⁻³ and $N_D=4.05 \times 10^{16}$ cm⁻³. The $N_D=0$ cm⁻³ case corresponds to the two control wafers, while the other two curves relate to the two compensated wafers. The plot again reveals the good agreement with *Klaassen's* model.

4.2. Minority carrier conductivity mobility

The minority carrier mobility was measured using the Sproul method on samples with mechanically abraded surfaces.[29] This method only requires a knowledge of two quantities, the effective lifetime τ and the thickness W of the sample. Due to the very high surface recombination velocity the lifetime is dominated in low injection by the diffusion rate of the minority carriers to the surface. For the case of an infinite surface recombination velocity, the relation between the effective lifetime (τ_{eff}), the diffusion coefficient (D_n), the sample thickness (W) and bulk lifetime (τ_b) is:[29]

$$\frac{1}{\tau_{eff}} = \frac{1}{\tau_b} + \left(\frac{\pi}{W} \right)^2 D_n \quad (1)$$

Knowing the thickness and the effective lifetime one can therefore deduce the electron diffusion coefficient. Because some of our samples have quite low resistivity, with low bulk lifetime, the diffusion constant was determined from the slope of a plot of $1/\tau$ vs $(\pi/W)^2$ using samples of different thickness, as explained by *Sproul et al.*[29] This allows the impact of the bulk lifetime to be eliminated from the analysis. The fit for a compensated sample of resistivity 1.6 Ωcm and non-compensated sample of resistivity 1.2 Ωcm is shown in Figure 3. The resulting electron mobilities are listed in Table I. There is a significant 35-45% reduction of electron mobility in our compensated silicon samples compared to the non-compensated silicon samples with similar net doping.

Figure 5 shows the minority electron mobilities plotted as a function of N_A , in analogy to Figure 4. While the control samples are in reasonable agreement with *Klaassen's* model, the compensated samples lie well below the curves predicted by it.

5. Hall Factor in compensated silicon

The Hall factor depends on the carrier type, the dominant scattering mechanisms, temperature and the magnitude of the magnetic field. The Hall factor approaches unity when the magnetic field is strong.[30] However, for practical reasons it is often difficult to measure under such high magnetic fields. Therefore it is of fundamental importance to measure the Hall factor r_H in compensated silicon in order to be able to convert low-field Hall mobilities into conductivity mobilities. Moreover the Hall factor is larger than 1 in n-type silicon and smaller than 1 in p-type silicon.[30] This raises uncertainty about the value of the Hall factor when both dopant types are present in the bulk, as is the case for compensated silicon.

The relationship between the Hall mobility μ_H and the conductivity mobility μ_C is expressed as $\mu_H = r_H \mu_C$. The resistivity has no part in the determination of the Hall factor, and thus the Hall factor can also be expressed as the ratio of the conductivity carrier density $p_{0,C}$ over the Hall carrier density $p_{0,H}$ as follows: $r_H = p_{0,C}/p_{0,H}$. Using the

Q-cells and Bart Geerligs of ECN for kindly supplying the wafers used in this study. Thanks are also due to Chris Samundsett for assisting with sample preparation and to Martin Wolf for helping with the ECV measurements.

References

- [1] S. Reggiani, M. Valdinoci, L. Colalongo, M. Rudan, G. Baccarani, A. D. Stricker, F. Illien, N. Felber, W. Fichtner and L. Zullino, *IEEE Transactions on Electron Devices* 49 (2002) 490 - 499.
- [2] D. B. M. Klaassen, *Solid-State Electronics* 35 (1992) 961 - 967.
- [3] D. B. M. Klaassen, *Solid-State Electronics* 35 (1992) 953 - 959.
- [4] G. Masetti, M. Severi and S. Solmi, *IEEE Transactions on Electron Devices* 30 (1983) 764 - 769.
- [5] N. D. Arora, J. R. Hauser and D. J. Roulston, *IEEE Transactions on Electron Devices* 29 (1982) 292 - 295.
- [6] J. M. Dorkel and P. Leturcq, *Solid-State Electronics* 24 (1981) 821 - 825.
- [7] W. R. Thurber, R. L. Mattis, Y. M. Liu and J. J. Filliben, *Journal of the Electrochemical Society* 127 (1980) 2291 - 2294.
- [8] W. R. Thurber, R. L. Mattis, Y. M. Liu and J. J. Filliben, *Journal of the Electrochemical Society* 127 (1980) 1807 - 1812.
- [9] D. M. Caughey and R. E. Thomas, *Proceedings of the Institute of Electrical and Electronics Engineers* 55 (1967) 2192 - 2193.
- [10] F. E. Rougieux, D. Macdonald, A. Cuevas, S. Ruffell, J. Schmidt, B. Lim and A. P. Knights, *Journal of Applied Physics* 108 (2010) 013706.
- [11] D. Macdonald, F. Rougieux, A. Cuevas, B. Lim, J. Schmidt, M. Di Sabatino and L. J. Geerligs, *Journal of Applied Physics* 105 (2009) 093704.
- [12] J. Veirman, S. Dubois, N. Enjalbert, J. P. Garandet, D. R. Heslinga and M. Lemiti, *Solid-State Electronics* 54 (2010) 671 - 674.
- [13] B. Lim, A. Liu, D. Macdonald, K. Bothe and J. Schmidt, *Applied Physics Letters* 95 (2009) 232109.
- [14] K. Peter, R. Kopecek, A. Soiland and E. Enebak, *Proceedings of the 23rd European Photovoltaic Solar Energy Conference*, Valencia, Spain (2008)
- [15] S. Dubois, N. Enjalbert and J. P. Garandet, *Applied Physics Letters* 93 (2008) 032114.
- [16] J. Libal, S. Novaglia, M. Acciarri, S. Binetti, R. Petres, J. Arumughan, R. Kopecek and A. Prokopenko, *Journal of Applied Physics* 104 (2008) 104507.
- [17] S. Pizzini and C. Calligaris, *Journal of the Electrochemical Society* 131 (1984) 2128 - 2132.
- [18] L. M. Falicov and M. Cuevas, *Physical Review* 164 (1967) 1025 - 1032.
- [19] M. Cuevas, *Physical Review* 164 (1967) 1021 - 1024.
- [20] M. B. Prince, *Physical Review* 92 (1953) 681 - 687.
- [21] J. Kraiem, R. Einhaus and H. Lauvray, *Proceedings of the 34th IEEE Photovoltaic Specialists Conference*, Philadelphia, USA (2009)
- [22] W. Krühler, C. Moser, F. W. Schulze and H. Aulich, *Proceedings of the 8th European Photovoltaic Solar Energy Conference*, Florence, Italy (1988) 1181-1185.
- [23] F. J. Morin and J. P. Maita, *Physical Review* 96 (1954) 28 - 35.
- [24] C. Jacoboni, C. Canali, G. Ottaviani and A. A. Quaranta, *Solid-State Electronics* 20 (1977) 77 - 89.
- [25] L. C. Linares and S. S. Li, *Journal of the Electrochemical Society* 128 (1981) 601 - 608.
- [26] D. Macdonald, A. Cuevas and L. J. Geerligs, *Applied Physics Letters* 92 (2008) 202119.
- [27] L. Van der Pauw, *Philips Technical Review* 20 (1958) 221 - 224.
- [28] R. Bock, P. Altermatt and J. Schmidt, (2008)
- [29] A. B. Sproul, M. A. Green and A. W. Stephens, *Journal of Applied Physics* 72 (1992) 4161 - 4171.
- [30] J. F. Lin, S. S. Li, L. C. Linares and K. W. Teng, *Solid-State Electronics* 24 (1981) 827 - 833.
- [31] D. K. Schroder, T. T. Braggins and H. M. Hobgood, *Journal of Applied Physics* 49 (1978) 5256 - 5259.
- [32] F. Padovani, *Journal of Applied Physics* 43 (1972) 2003 - 2005.